Thermodynamic and Structural Characterization of Amphiphilic Melamine-type Monolayers

D. Vollhardt,*,† V. B. Fainerman,‡ and F. Liu†,§

Max-Planck Institute of Colloids and Interfaces, D-14424 Potsdam/Golm, Germany, Medical Physicochemical Centre, Donetsk Medical University, 16 Ilych Avenue, Donetsk 340003, Ukraine, and Department of Chemistry, Institute of Coordination Chemistry, Nanjing University, Nanjing 210093, P. R. China

Received: February 15, 2005; In Final Form: April 15, 2005

Monolayers of amphiphilic melamine derivatives are good candidates for the formation of supramolecular structures by hydrogen-bonding of nonsurface active species dissolved in the aqueous subphase by molecular recognition. In the present work, the thermodynamic and structural properties of the Langmuir monolayers of a homologous series of a selected amphiphilic melamine-type are characterized. Good candidates for such studies are the decyl, undecyl, and dodecyl homologues of the 2,4-di(*n*-alkylamino)-6-amino-1,3,5-triazine ($2C_nH_{2n+1}$-melamine) monolayers because of their two-phase coexistence region in the accessible temperature range. The characterization of the structural and phase behavior is performed by a combination of surface pressure studies with Brewster angle microscopy (BAM) imaging and Grazing incidence X-ray diffraction (GIXD) measurements. A comprehensive thermodynamic analysis provides good agreement between the experimental surface pressure − area (Π-A) isotherms and the theoretical curves that were calculated on the basis of equations of state for a large region of monolayer stages developed by us in *J. Phys. Chem.* **1999**, *103*, 145. Theoretical curves calculated by application of equations of state only for the fluid monolayer state proposed recently by Rusanov (*J. Chem Phys.* **2004**, *120*, 10736) are in good agreement with the experiments in a limited temperature range. A rigorous equation is derived and applied to the experimental results for the calculation of the enthalpy of two-dimensional phase transition. The combination of BAM and GIXD illustrates that the microscopic long range ordering of the condensed monolayer phases is related to the lattice structure of the condensed monolayer.

Introduction

There is current interest in host−guest structures and supramolecular chemistry such as the design and synthesis of enzyme mimics, selective molecular recognition of biorelevant species, etc.[1,2] Langmuir monolayers have received considerable attention to study interfacial molecular recognition and to construct supramolecular assemblies of specific molecular composition.[3,4] Such interfacial molecular recognition models have been studied to mimic biological-medical recognition processes or to develop miniaturized sensors.[5−7] Generally, these models consist of a amphiphilic host monolayer that recognizes a nonsurface active guest component dissolved in the aqueous subphase. Hydrogen bonds play an important role in the formation of highly ordered molecular architectures because of its directional preference and specific interaction.[8,9]

For designing supramolecular assemblies in organic media and in the solid state, the combination of derivatives of melamine and barbiturate on the basis of hydrogen bonding has been effective.[10−12] With this in view, amphiphilic melamine derivatives have been successfully applied as *host*-monolayers for interfacial molecular recognition of barbituric acid dissolved in the aqueous subphase.[13,14] It was shown that in this system, supramolecular networks of linearly extended hydrogen-bondings are formed at the air/water interface.

So far, the major activities in the field of interfacial molecular recognition have been directed to design mimetic systems and provide evidence for the guest binding dissolved in the aqueous subphase at the host monolayer.[4,15,16] On the other hand, there is nearly no knowledge about the phase and structural properties of the amphiphilic melamine-type monolayers and in which way these are affected by molecular recognition of a guest component dissolved in the aqueous subphase.

The objective of the present work is to characterize the thermodynamic and structural properties of the Langmuir monolayers of a homologous series of a selected amphiphilic melamine-type. The decyl, undecyl, and dodecyl homologues of the 2,4-di(*n*-alkylamino)-6-amino-1,3,5-triazine ($2C_nH_{2n+1}$-melamine) monolayers show a two-phase coexistence region in the accessible temperature range so that they are good candidates for the studies. The characterization of the structural and phase behavior has been performed by a combination of surface pressure studies with Brewster angle microscopy (BAM) imaging and Grazing incidence X-ray diffraction (GIXD) measurements.

Experimental Section

Materials. Systematic studies of the phase and structural features of an amphiphilic melamine-type monolayer require the availability of a homologous series. Therefore, we synthesized ($2C_nH_{2n+1}$-melamine) with alkyl chain lengths $C_{10}H_{21}$, $C_{11}H_{23}$, $C_{12}H_{25}$, $C_{14}H_{29}$, and $C_{16}H_{33}$. Figure 1 shows the chemical structure of 2,4-di(*n*-undecylamino)-6-amino-1,3,5-triazine ($2C_{11}H_{23}$-melamine).

* To whom correspondence should be addressed.
† Max-Planck Institute of Colloids and Interfaces.
‡ Donetsk Medical University.
§ Nanjing University.

10.1021/jp050796u CCC: $30.25
Published on Web 05/25/2005

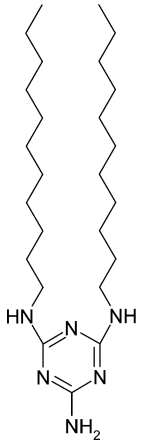

Figure 1. Chemical structure of 2,4-di(*n*-undecylamino)-6-amino-1,3,5-triazine ($2C_{11}H_{23}$-melamine).

In the first step, 2-amino-4,6-dichloro-1,3,5-triazine was prepared according to ref 11. Ammonia (NH_3) was slowly bubbled into a slurry of cyanuric chloride (36.88 g, 0.2 mol) and diglyme (30 mL) in dioxane (230 mL) cooled in an ice−water bath ($T < 10$°C). The addition of NH_3 was stopped after about 2 h when 6.8 g (0.4 mol) had been taken up by the mixture. Excess NH_3 was removed by blowing nitrogen through the reaction flask. After filtration, the precipitate was washed well with THF. The collected solutions were concentrated by rotary evaporation and the solid residue was dried under vacuum yielding 29.5 g of a white powder, mp 218 °C. The obtained 2-amino-4,6-dichloro-1,3,5-triazine was directly used to synthesize the homologous 2,4-di(*n*-alkylamino)-6-amino-1,3,5-triazines ($2C_nH_{2n+1}$-melamine) by aminoalkylation.[17] A mixture of 6 mmol of 2-amino-4,6-dichloro-1,3,5-triazine, 12.7 mmol of $C_{11}H_{23}NH_2$, and 12.7 mmol of $NaHCO_3$in 100 mL of anhydrous dioxane was stirred under reflux for 30 h. The precipitate was removed by filtration and washed with dioxane. After removing the solvent by rotary evaporation a pale-yellow solid was obtained. Recrystallization in ethanol and heptane resulted in a white final product (purity >99%).

Ultrapure water produced by "Purelab Plus" was used as subphase.

Isotherm and BAM Measurements. The surface pressure−area (Π−A) isotherms of the amphiphilic melamine-type monolayers spread on pure water were measured in the accessible temperature range with a reproducibility of ±0.1 mN/m.[18] Imaging of the monolayers was performed with a Brewster angle microscope (BAM 2, NFT, Göttingen) coupled to the film balance. The microscope was equipped with a special scanning technique for providing sharp images. To obtain BAM images real in scale and angle, the CCD sensor of the camera is tilted according to the Scheimpflug condition. The application of a green laser (Uniphase, San Jose, CA) allowed a resolution of the BAM images of approximately 3 μm.

GIXD Measurements. The grazing incidence X-ray diffraction (GIXD) experiments were performed using the liquid−surface diffractometer on the undulator beamline BW1 at HASYLAB, DESY, Hamburg, Germany. The Langmuir trough was located in a sealed He flushed container to reduce the background in the X-ray scattering experiments. A monochromatic synchrotron X-ray beam was adjusted to strike the helium/water interface at a grazing incidence angle $\alpha_i = 0.85\alpha_c$, where α_c is the critical angle for total reflection. The diffracted intensity is detected by a linear position-sensitive detector (PSD) (OED-100-M, Braun, Garching, Germany) as a function of the vertical scattering angle α_f. To record the intensity as a function of the horizontal scattering angle $2\theta_{xy}$ the detector was rotated around the sample. The in-plane divergence of the diffracted beam was restricted to 0.09° by a Soller collimator in front of the PSD. The scattering vector Q has an in-plane component $Q_{xy} \approx (4\pi/\lambda) \sin \theta_{xy}$ and an out-of-plane component $Q_z \approx (2\pi/\lambda) \sin \alpha_f$, where λ is the X-ray wavelength.[19,20] The intensities as a function of Q_{xy} and Q_z were least-squares fitted as a Lorentzian in the in-plane direction and as a Gaussian in the out-of-plane direction The lattice parameters are obtained from the peak positions. The lattice spacing is given by $d(hk) = 2\pi/Q_{xy}^{hk}$, where (h,k) denotes the order of the reflection. The polar tilt angle t of the long molecule axis, and the tilt azimuth ψ_{xy} are calculated from the positions of the Q_{xy} and Q_z maxima,[21] according to $Q_z^{hk} = Q_{xy}^{hk} \cos \psi_{hk} \tan t$. The lattice parameters $a,b,$ and γ were calculated from the lattice spacing d_{hk} and from these the unit cell area $A_{xy} = ab \sin \gamma$. The cross section per alkyl chain $A_0 = A_{xy} \cos t$ is related to the unit cell area A_{xy} (area per molecule parallel to the interface) and the tilt angle t.

Theory

For processing the Π−A isotherms, the theoretical model recently developed by us has been used.[22]

The equation of state for monolayers in the fluid (G or LE) state is represented by Volmer's equation[23,24]

$$\Pi = \frac{1}{m}\frac{kT}{A-\omega} - \Pi_{coh} \tag{1}$$

The equation of state for the fluid/condensed phase coexistence region ($A < A_c$) has been derived on the basis of the generalized Volmer's equation (see refs 22−24)

$$\Pi = \frac{1}{m}\frac{kT\alpha\beta}{A-\omega[1+\epsilon(\alpha\beta-1)]} - \Pi_{coh} \tag{2}$$

In these equations, Π is the surface pressure, k is the Boltzmann constant, T is the temperature, ω is the partial molecular area for monomers (or the limiting area of molecule in the gaseous state), A is the area per molecule, A_c is the molecular area which corresponds to the onset of the phase transition (i.e., at $\Pi = \Pi_c$), m is the aggregation number for small aggregates, and Π_{coh} is the cohesion pressure, which accounts for the intermolecular interaction The parameter α expresses the dependence of the aggregation constant on the surface pressure

$$\alpha = \frac{A}{A_c}\exp\left[-\epsilon\frac{\Pi-\Pi_c}{kT}\omega\right] \tag{3}$$

and β is the fraction of the monolayer free from aggregates, $\beta = \alpha$, as $A_c < 2\omega$;[25] where $\epsilon = 1 - \omega_{cl}/\omega$, and ω_{cl} is the area per monomer in a cluster.

The area per molecule in the aggregate can be different from the limiting area per molecule in the gaseous state. This fact is accounted for by the parameter $\epsilon = \epsilon_0 + \eta\Pi$[25]

$$\omega_{cl} = \omega(1-\epsilon) = \omega(1-\epsilon_0-\eta\Pi) \tag{4}$$

where ϵ_0 is a relative jump of the area per molecule and η is a relative two-dimensional compressibility of the condensed monolayer.

Very recently, Rusanov[26] has published equations of state for the fluid (G, LE) state of Langmuir monolayers. It is interesting to note that all his equations of state are based on his eq 50 that is identical to eq 5 of our paper[23] published already

in 1999. Equation 5 of our paper[23] has been written in differential form, whereas eq 50 of his paper is written in integral form.

We used the first approximation for the solution of this equation which we called Volmer equation. Such an approximation is also used by Rusanov and he obtained similar to eq 1 of this paper (with $m = 1$)[23] eq 69 of his paper.[26] Rusanov derived as higher approximations the following general equation of state for the fluid (G and LE) state (eq 84 of ref 26):

$$\Pi = \frac{kT}{\omega_1}\frac{\varphi}{(1-k_0\varphi)^{n-1}}\left\{1 - \frac{2nk_0 - 2k_0 - 4}{(n-1)(n-2)k_0^2\varphi}[(1 - k_0\varphi)^{n-1} - 1 + (n-1)k_0\varphi]\right\} - \Pi_{coh} \quad (5)$$

where $\varphi = \omega_1/A$, $n \geq 3$, and k_0 is a constant. For the determination of k_0, the data of Erpenbeck and Luban[27] (Monte Carlo and molecular dynamic methods for hard disks) were used in ref 26. The best fit of eq 5 to the data of ref 27 is achieved with $k_0 = 1.0145$. With this k_0 value at $n = 3$, eq 5 takes the form

$$\Pi = \frac{kT}{\omega_1}\frac{\varphi(1 - 0.029\varphi)}{(1 - 1.0145\varphi)^2} - \Pi_{coh} \quad (6)$$

It is possible to accept $k_0 = 1$ almost without a mistake in eqs 5 and 6. This results in the known scaled particle theory (SPT) equation[28,29]

$$\Pi = \frac{kT}{\omega_1}\frac{\varphi}{(1-\varphi)^2} - \Pi_{coh} \quad (7)$$

For the calculation of the enthalpy of the two-dimensional phase transition, we generalized the theory presented in ref 30. Introducing eq 11 of ref 30

$$\frac{dx}{dT} = x\frac{d(\Delta G^0/RT)}{dT} \quad (8)$$

into eq 10 of ref 30

$$\frac{d\Pi}{dT} = \left(\frac{d\Pi}{dT}\right)_x + \left(\frac{d\Pi}{\partial x}\right)\frac{dx}{dT} \quad (9)$$

and using the Gibbs−Helmholtz equation

$$\frac{\partial}{\partial T}\left(\frac{\Delta G}{RT}\right) = -\frac{\Delta H}{RT^2} \quad (10)$$

one obtains the equation for the standard enthalpy of two-dimensional phase transition $\Delta H°$

$$\Delta H° = -\frac{RT^2}{x}\frac{d\Pi_c/dT}{d\Pi_c/dx} = -\frac{RT^2}{x}\frac{dx}{dT} \quad (11)$$

where $x = \omega_{cl}/A_c$, R is the gas constant, and $\Delta G°$ is the variation of the standard (Gibbs) free energy of the two-dimensional phase transition. Equation 11 is more rigorous than eq 16 deduced in ref 30 as for the derivation of eq 11 Volmer's equation of state is not used.

Results and Discussion

For the thermodynamic characterization of the monolayers, surface pressure−area (Π−A) isotherms of the homologous $2C_nH_{2n+1}$-melamines have been studied for different temperatures in the accessible range. As known, the precondition for the development of well-shaped two-dimensional morphology (domain textures) of the condensed phase is the existence of a "plateau" region in the Π−A isotherm at different temperatures in the accessible range that represents thermodynamically the coexistence between the fluid and the condensed state. For the homolgous $2C_nH_{2n+1}$-melamine series, this precondition is fulfilled only for the alkyl chain lengths $C_{10}H_{21}$, $C_{11}H_{23}$, and $C_{12}H_{25}$. To distinguish better between the isotherms experimentally measured and those calculated thermodynamically, the experimental Π−A isotherms are represented by symbols although they were recorded continuously. The symbols of Figure 2 show 5 Π−A isotherms of $2C_{10}H_{21}$-melamine mea-

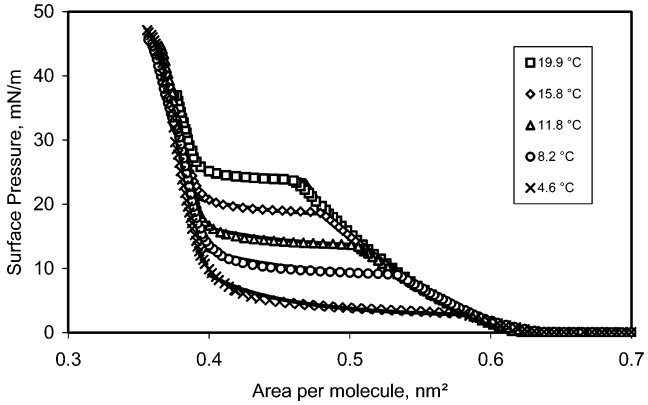

Figure 2. Π−A isotherms of $2C_{10}H_{21}$-melamine monolayers spread on water measured in the temperature range between 4.6 and 19.9 °C.

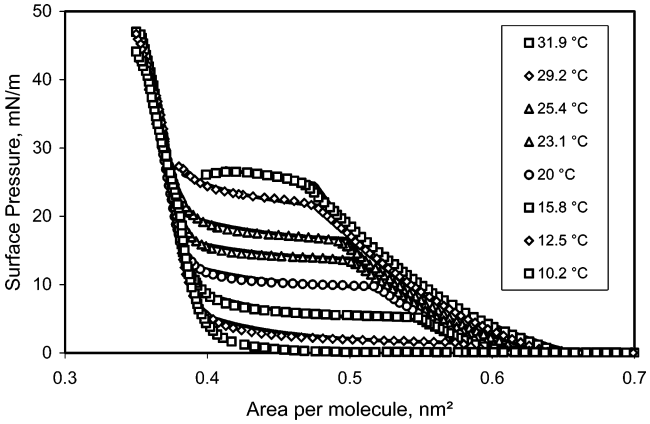

Figure 3. Π−A isotherms of $2C_{11}H_{23}$-melamine monolayers spread on water measured in the temperature range between 10.2 and 31.9 °C.

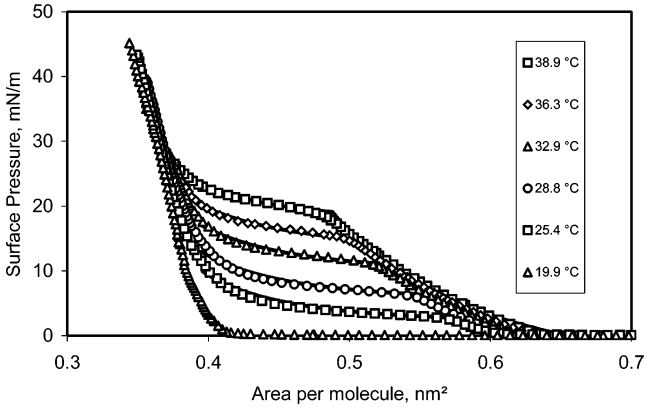

Figure 4. Π−A isotherms of $2C_{12}H_{25}$-melamine monolayers spread on water measured in the temperature range between 19.9 and 38.9 °C.

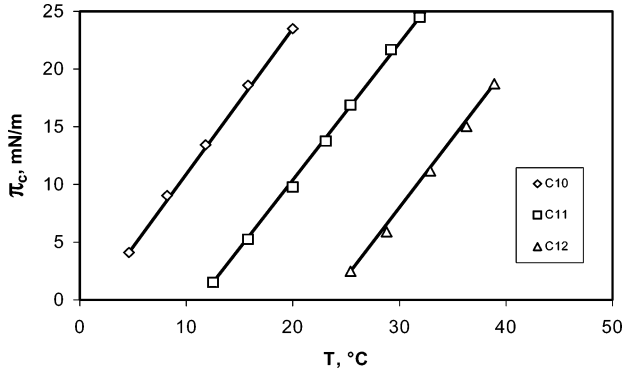

Figure 5. Temperature dependence of the phase transition pressure Π_c of the monolayers of $2C_{10}H_{21}$-melamine-, $2C_{11}H_{23}$-melamine, and $2C_{12}H_{25}$-melamine spread on water.

TABLE 1: Parameter Values of Eq 2 Calculated for $2C_{10}H_{21}$-Melamine Molayers at Different Temperatures

temperature, °C	4.6	8.2	11.8	15.8	19.9
ω_1, nm^2	0.36	0.36	0.36	0.36	0.36
A_c, nm^2	0.582	0.535	0.51	0.487	0.468
Π_{coh}, mN/m	13.8	16.45	17.2	16.35	17.6
ϵ_0	0.14	0.19	0.20	0.25	0.26
m	1.03	0.87	0.86	0.9	0.83
$-\Delta H°$, kJ/mol	10.6	10.8	10.4	9.2	9.9

TABLE 2: Parameter Values of Eq 2 Calculated for $2C_{11}H_{23}$-Melamine Monolayers at Different Temperatures

temperature, °C	12.5	15.8	20.0	23.1	25.4	29.2	31.9
ω_1, nm^2	0.36	0.36	0.36	0.36	0.36	0.36	0.35
A_c, nm^2	0.58	0.55	0.52	0.504	0.498	0.484	0.476
Π_{coh}, mN/m	16.2	15.7	16.6	16.6	16.6	15.6	18.4
ϵ_0	0.19	0.18	0.22	0.24	0.22	0.21	0.18
m	1.00	1.02	0.97	0.93	0.91	0.91	0.72
$-\Delta H°$, kJ/mol	8.9	8.8	8.5	8.4	8.2	8.1	8.0

TABLE 3: Parameter Values of Eq 2 Calculated for $2C_{12}H_{25}$-Melamine Molayers at Different Temperatures

temperature, °C	25.4	28.8	32.9	36.3	38.9
ω_1, nm^2	0.36	0.36	0.36	0.36	0.36
A_c, nm^2	0.566	0.545	0.522	0.506	0.488
Π_{coh}, mN/m	15.9	16.5	16.6	15.9	14.8
ϵ_0	0.14	0.14	0.15	0.18	0.19
m	1.05	0.98	0.95	0.96	1.0
$-\Delta H°$, kJ/mol	10.9	10.7	10.5	10.2	10.1

sured between 4.6 and 19.9 °C, the symbols of Figure 3 show 8 Π−A isotherms of $2C_{11}H_{23}$-melamine between 10.2 and 31.9 °C, and the symbols of Figure 4 show 6 Π−A isotherms of $2C_{12}H_{25}$-melamine between 19.9 and 38.9 °C. Over the whole temperature range studied, all three homologues form a two-phase coexistence region, the extent of which decreases clearly as the temperature increases. In this respect, the $2C_nH_{2n+1}$-melamine monolayers spread on water behave thermodynamically as usual amphiphilic monolayers.[18] In the case of $2C_{11}H_{23}$-melamine, the monolayer collapses at the end of the two-phase coexistence region at 31.9 °C.

Additional information on the phase behavior and the thermodynamic characteristics of the transition between the fluid and condensed phase can be obtained from the temperature dependence of the phase transition point Π_c (the kink point in the Π−A isotherm at onset of the phase transition). The symbols of Figure 5 show the experimental Π_c−T dependence for the three homologous melamine amphiphiles $2C_{10}H_{21}$-melamine, $2C_{11}H_{23}$-melamine, and $2C_{12}H_{25}$-melamine. Furthermore, it can be seen that the fluid/condensed phase coexistence region of the homologous melamine amphiphiles with the alkyl chain

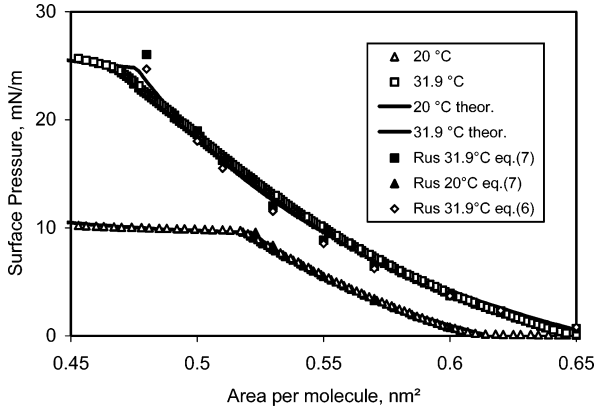

Figure 6. Comparison of the theoretical curves obtained with eq 1 derived by the authors and obtained with eqs 6 and 7 derived by Rusanov with the experimental Π−A isotherms of $2C_{11}H_{23}$-melamine monolayers spread on water at 20 and 31.9 °C.

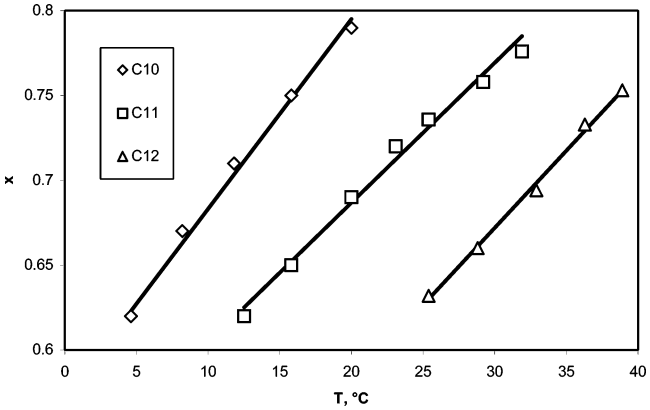

Figure 7. Temperature dependence of the parameter $x = \omega_{cl}/A_c$ of the monolayers of $2C_{10}H_{21}$-melamine-, $2C_{11}H_{23}$-melamine, and $2C_{12}H_{25}$-melamine spread on water.

lengths between $C_{10}H_{21}$ and $C_{12}H_{25}$ is in the measurable temperature range, and it can be concluded to which temperature range inaccessible to the used measuring conditions the fluid/condensed phase coexistence is shifted with the change of the alkyl chain length. Already for the monolayers of $2C_{13}H_{27}$-melamine and those with still larger alkyl chain length, the phase coexistence region must be expected at such high temperatures that for these homologues reasonable BAM studies of the domain morphology are impossible.

The solid lines of Figures 2-4 represent the theoretical curves obtained on the basis of the equations of state eqs 1 and 2. The corresponding parameters of the isotherms are listed in Tables 1−3.

The calculated values show that at condensation ($\epsilon_0 > 0$) the area per molecule A_c decreases for the monolayers of all three melamine-type homologues. It is interesting to mention that the aggregation number for small aggregates mexisting in the fluid state at $A > A_c$, also decreases as the temperature increases. In the case that $m \approx 1$, monomers exist, whereas the case $m < 1$ indicates relative freedom of the two alkyl chains of the melamine-type amphiphiles.

For comparison, we used eq 7 derived by Rusanov on the basis of his generalized equation of state for the calculation of theoretical curves of the fluid (G and LE) state in the region $A > A_c$. The results can be seen in Figure 6. The filled symbols has been calculated using eq 7 for two temperatures:

20 °C, $\omega_1 = 0.337$ nm^2, $\Pi_{coh} = 11.0$ mN/m;

31.9 °C, $\omega_1 = 0.34$ nm^2, $\Pi_{coh} = 9.0$ mN/m.

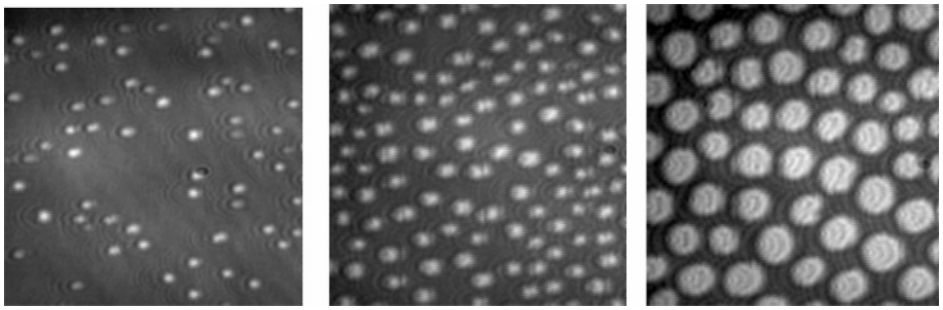

Figure 8. Domain growth within the plateau region of the Π−A isotherm of $2C_{11}H_{23}$-melamine monolayers spread on water; $T = 20$ °C; image size 200 × 200 μm.

As can be seen, only at the temperature of 20 °C the theoretical values calculated on the basis of eq 7 coincides with the experimental results and the theoretical curve obtained on the basis of eq 1 derived by us in ref 23. On the other hand, at the higher temperature (31.9 °C), at which the fluidlike (LE, G) state can attain high surface pressure values (>26 mN/m at 31.9 °C), the difference to the real experimental results is rather large. Nevertheless, the deviation of the real experiment is smallest using the submitted parameters of eq 7. That means the difference to the experimental results cannot improved by using other parameter values. On the contrary, in this case, the mistake is increased even more. The agreement with the experiments can also not be improved if the calculations are performed on the basis of the exact Rusanov's equation (eq 6) (see eqs 84 or 89 of ref 26). The corresponding open symbols Rus 31.9 °C eq 6 of Figure 6 shows calculated values for 31.9 °C with $\omega_1 = 0.367$ nm^2 and $\Pi_{coh} = 13.5$ mN/m. As can be seen, the results are not better than in the case of the approximate eq 7 because of the insignificant difference between eqs 6 and 7.

Equation 11, which is more rigorously derived than an equation previously obtained,[30] is used to calculate the enthalpy for the two-dimensional phase transition. At first, the values of $x = \omega_{cl}/A_c$ must be calculated using the experimental values of A_c, and $\omega_{cl} = 0.36$ nm^2 for the three homologous melamine amphiphiles $2C_{10}H_{21}$-melamine, $2C_{11}H_{23}$-melamine, and $2C_{12}H_{25}$-melamine and temperatures. Figure 7 illustrates that, similar to the linear Π_c(T) dependence (see Figure 5), x depends also linearly from T for all three melamine homologues having similar dx/dT values. Therefore, for the calculation of $\Delta H°$, a constant dx/dT value for each melamine homologue can be used. Correspondingly, the $\Delta H°$ values (see Tables 1−3) are rather similar for the three homologous melamine amphiphiles $2C_{10}H_{21}$-melamine, $2C_{11}H_{23}$-melamine, and $2C_{12}H_{25}$-melamine and temperatures.

The Brewster angle microscopy (BAM) provides information about the long-range ordering in microscopic scale. Figures 2−4 illustrate that, in the comparison to the other homologous melamine-type amphiphiles, the fluid/condensed phase coexistence region of the $2C_{11}H_{23}$-melamine monolayers occurs over a large temperature interval in the measurable region. Therefore, the BAM results of $2C_{11}H_{23}$-melamine are selected for the presentation.

Figure 8 shows a sequence of typical BAM images during the domain growth in the plateau region of the $2C_{11}H_{23}$-melamine monolayer spread on water at 20 °C.

First numerous very small condensed phase domains appear at areas less smaller than the main phase transition point A_c. At further compression, the domains grow within the "plateau" region of the $\pi-A$ isotherm to an average size of approximately 10−25 μm in diameter. The small domain size and the formation of a large number of them after the phase transition point indicates a high nucleation rate. A certain difference in the size of the grown domains near the end of the plateau suggests a progressive nucleation mechanism. The compact domains are not regularly shaped, also never really round. Therefore, the line tension seems to be rather small. An inner texture does not occur. The domains are rather tightly packed without touching each other at the end of the "plateau" of the isotherm.

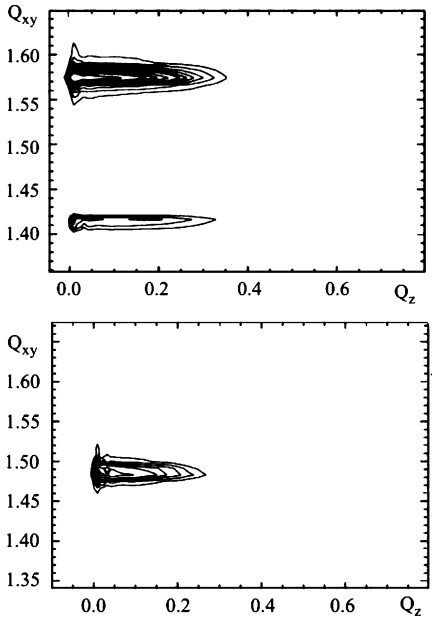

Figure 9. GIXD contour plots of a $2C_{11}H_{23}$-melamine monolayer spread on water at $\Pi = 11$ mN/m (top) $T = 5$ °C, (bottom) $T = 20$ °C.

TABLE 4: Lattice Parameters of $2C_{11}H_{23}$-melamine Monolayers Spread on Water at 5 °C

Π (mN/m)	a (nm)	b (nm)	A_{xy} (nm^2)	A_0 (nm^2)	t (deg)	γ (deg)	tilt direction
1.5	0.447	0.499	0.1994	0.1984	6.0	116.6	NNN
5	0.447	0.498	0.1989	0.1980	5.3	116.7	NNN
10	0.446	0.498	0.1986	0.1978	5.2	116.6	NNN
30	0.443	0.494	0.1955	0.1953	2.5	116.7	NNN
40	0.442	0.492	0.1943	0.1941	2.4	116.7	NNN

GIXD experiments were performed to study whether lattice structures are formed by $2C_{11}H_{23}$-melamine monolayers spread on water and in which way they are affected by temperature change. The contour plots of the corrected diffraction intensities as a function of the in-plane (Q_{xy}) and out-of-plane (Q_z) components of the scattering vectors of the $2C_{11}H_{23}$-melamine monolayers spread on water are presented in Figure 9. The corresponding structure data calculated for different surface pressures are listed in Table 4 for $T = 5$ °C and in Table 5 for $T = 20$ °C, wherein a, b, and γ are the unit cell parameters, A_{xy}

TABLE 5: Lattice Parameters of $2C_{11}H_{23}$-Melamine Monolayers Spread on Water at 20 °C

Π (mN/m)	*a* (nm)	A_0 (nm^2)	*t* (deg)	γ (deg)
11	0.488	0.2062	0	120
12	0.488	0.2062	0	120
20	0.487	0.2054	0	120
30	0.485	0.2037	0	120

is the in-plane molecule area, *t* is the polar tilt angle, and A_0 is the cross-section area of alkyl chain.

The reflexes of the contour plots indicate different lattice types for the two temperatures. The contour plot measured at a relatively low temperature ($T = 5$ °C) shows two reflexes with both maxima at $Q_z > 0$ characteristic of a centered rectangular lattice and alkyl chains are tilted toward their next nearest neighbor (NNN) direction (Figure 9). However, the tilt of the alkyl chains is rather small. At higher temperatures ($T = 20$ °C), the contour plot has only one reflex with the maximum at $Q_z = 0$, that means, in this case the $2C_{11}H_{23}$-melamine monolayer has a hexagonal lattice, the alkyl chains are normally erected, so that the polar tilt t is zero. According to earlier work, the microscopic textural features of the condensed monolayer phases are related to the lattice structure of the condensed monolayer. The hexagonal lattice structure obtained at 20 °C is an agreement with the absence of an inner texture as observed in the condensed phase domains (see Figure 8). An inner texture can exist only if the alkyl chains of the monolayer are tilted.

Conclusions

Monolayers of amphiphilic melamine derivatives are good candidates to design mimetic systems in the field of interfacial molecular recognition. They are highly effective as host monolayers to form supramolecular structures by molecular recognition by complementary hydrogen-bonding of nonsurface active species dissolved in the aqueous subphase. In the present work, the decyl, undecyl, and dodecyl homologues of the 2,4-di(*n*-alkylamino)-6-amino-1,3,5-triazine ($2C_nH_{2n+1}$-melamine) monolayers have been studied to obtain first information about the thermodynamic and structural properties of the host monolayers spread on water. These alkyl chain lengths are best-suited for the studies because the monolayers of these homologues have the two-phase coexistence region in the accessible temperature range. The combination of surface pressure studies with Brewster angle microscopy (BAM) imaging and Grazing incidence X-ray diffraction (GIXD) measurements is optimal for characterizing the structural features and phase behavior of the melamine-type monolayers. A comprehensive thermodynamic analysis has been performed on the basis of equations of state for a large region of monolayer stages developed by us in *J. Phys. Chem.* **1999**, *103*, 145. It was found that the theoretical curves are in good agreement with the experimental surface pressure−area (Π−A) isotherms for all three homologues over the whole measured temperature range. The theoretical curves calculated by application of equations of state only for the fluid monolayer state proposed recently by Rusanov (*J. Chem Phys.* **2004**, *120*, 10736) are only in good agreement with the experiments in a limited temperature range. For the calculation of the enthalpy of two-dimensional phase transition, a new rigorous equation is derived and applied to the experimental results. In the case of molecular recognition systems where only very small quantities of the components are available, the thermodynamic analysis can be performed on the basis of a drop shape analysis instead of film balance measurements.[31]

The microscopic long-range ordering of the condensed monolayer phases becomes understandable by the results of the lattice structure of the condensed monolayer. The hexagonal lattice structure does not allow the formation of an inner texture within the condensed phase domains.

Acknowledgment. Financial support from the Deutsche Forschungsgemeinschaft (DFG Grant VO-710/7-1) is gratefully acknowledged.

References and Notes

(1) Philip. D.; Stoddart, J. F. *Angew. Chem., Int. Ed. Engl.* **1996**, *35*, 1154.
(2) Murakami, Y.; Kikuchi, J.; Hisaeda, Y.; Hayashida, O. *Chem. Rev.* **1996**, *96*, 721.
(3) Kunitake, T. *Thin Solid Films* **1996**, *284/285*, 9.
(4) Ariga, K.; Kunitake, T. *Acc. Chem. Res.* **1998**, *31*, 371.
(5) Ringsdorf, H.; Schlarb, B.; Venzmer, J. *Angew. Chem., Int. Ed. Engl.* **1989**, *27*, 113.
(6) Kunitake, T. *Angew. Chem., Int. Ed. Engl.* **1992**, *31*, 706.
(7) Shimomura, M.; Nakamura, F.; Ijiro, K.; Taketsuna, H.; Tanaka, M.; Nakamura, H.; Hasebe, K. *J. Am. Chem. Soc.* **1997**, *119*, 2341.
(8) Boschke, F. L., Ed.; Hydrogen bonds. In *Topics in Current Chemistry*; Springer-Verlag: Heidelberg, Germany, 1984; Vol. 120.
(9) Desiraju, G. R. *Angew. Chem.* **1995**, *107*, 2541.
(10) Zerkowski, J. A.; Mathias, J. P.; Whitesides, G. M. *J. Am. Chem. Soc.* **1994**, *116*, 4305.
(11) Zerkowski, J. A.; MacDonald, J. C.; Seto, C. T.; Wierda, D. A.; Whitesides G. M. *J. Am. Chem. Soc.* **1994**, *116*, 2382.
(12) Zerkowski, J. A.; Whitesides, G. M. *J. Am. Chem. Soc.* **1994**, *116*, 4298.
(13) Ebara, Y.; Itakura, K.; Okahata, Y. *Langmuir* **1996**, *12*, 5165.
(14) Matsuura, K.; Ebara, Y.; Okahata, Y. *Langmuir* **1997**, *13*, 814.
(15) Kurihara, K.; Kawahara, T.; Sasaki, D. Y.; Ohto, K.; Kunitake, T. *Langmuir* **1995**, *11*, 1408.
(16) Okahata, Y.; Ariga, K.; Tanaka, K. In *Thin Films Vol. 20. Organic Thin films and Surfaces: Directions for the Nineties*; Ulman, A., Ed.; Academic Press: New York, 1995; p 317.
(17) Koyano, H.; Bissel, P.; Yoshihara, K.; Ariga, K.; Kunitake, T. *Chem. Eur. J.* **1997**, *3*, 1077.
(18) Vollhardt, D. *Adv. Colloid Interface Sci.* **1996**, *64*, 143.
(19) Als-Nielsen, J.; Jacquemain, D.; Kjaer, K.; Leveiller, F.; Lahav, M.; Leiserowitz, L. *Phys. Rep.* **1994**, *246*, 251.
(20) Kjaer, K. *Physica B* **1994**, *198*, 100.
(21) Als-Nielsen, J.; Kjaer, K. In *Phase Transitions in Soft Condensed Matter*; Riste, T., Sherrington, D., Eds.; NATO ASI Series B.; Plenum Press: New York, 1989; Vol. 211, p 113.
(22) Vollhardt, D.; Fainerman, V. B. *J. Phys. Chem. B* **2004**, *108*, 297.
(23) Fainerman, V. B.; Vollhardt, D. *J. Phys. Chem. B* **1999**, *103*, 145.
(24) Vollhardt, D.; Fainerman, V. B.; Siegel, S. *J. Phys. Chem. B* **2000**, *104*, 4115.
(25) Fainerman, V. B.; Vollhardt, D. *J. Phys. Chem. B* **2003**, *107*, 3098.
(26) Rusanov, A. I. *J. Chem. Phys.* **2004**, *120*, 10736.
(27) Erpenbeck, J. J.; Luban, M. *Phys. Rev. A* **1985**, *32*, 2920.
(28) Helfand, E.; Frish, H. L.; Lebowitz, J. L. *J. Chem. Phys.* **1961**, *34*, 1037.
(29) Frish, H. L. *Adv. Chem. Phys.* **1964**, *6*, 229.
(30) Vollhardt, D.; Fainerman, V. B. *J. Phys. Chem. B* **2002**, *106*, 12000.
(31) Kwok, D. Y.; Vollhardt, D.; Miller, R.; Li, D.; Neumann, A. W. *Colloids Surf. A* **1994**, *88*, 51.